Available online at www.sciencedirect.com
SCIENCE DIRECT®
Engineering Structures 25 (2003) 1743–1753
ENGINEERING STRUCTURES
www.elsevier.com/locate/engstruct

Cyclic seismic testing of steel moment connections reinforced with welded straight haunch

Cheol-Ho Lee [a,*], Jong-Hyun Jung [b], Myoung-Ho Oh [c], En-Sook Koo [c]

[a] *Department of Architecture, Seoul National University, San 56-1, Shillim-Dong, Kwanak-Gu, Seoul 151-742, South Korea*
[b] *Department of Architectural Engineering, Kyungnam University, Wolyoung-Dong 449, Masan, 631-701, South Korea*
[c] *Hyundai Institute of Construction Technology, Mabuk-Ri, Goosung-Eup, Yongin-Shi, Gyunggi-Do 449-710, South Korea*

Received 17 February 2003; received in revised form 23 June 2003; accepted 2 July 2003

Abstract

A simplified seismic design procedure as well as force transfer model for seismic steel moment connections using a welded straight haunch was recently proposed. As a follow-up study, cyclic seismic testing was conducted to verify the proposed procedure and to develop strategies that would prevent cracking at the haunch tip. All the specimens based on the proposed procedure effectively pushed the plastic hinging of the beam outside the haunch and developed satisfactory connection ductility with no fracture. A sloped edge combined with a drilled hole near the haunch tip, or a pair of stiffeners that partially or fully extended from the beam web, successfully prevented crack initiation at the haunch tip. The strut action of the haunch web, which had been predicted from the previous analytical study, was also identified through the strain gage readings in this experiment.
© 2003 Elsevier Ltd. All rights reserved.

Keywords: Steel moment connections; Haunch; Cyclic seismic testing; Plastic hinge

1. Introduction

The 1994 Northridge and the 1995 Kobe earthquakes caused widespread brittle fracture in the connections of steel moment-resisting frames. As a response to the unexpected damage, a variety of new designs have been proposed. The more popular design strategies to resolve the problems associated with the connection damage included strengthening or weakening the beams that frame into the connection [1–7]. A combined strategy (or light rib reinforcement combined with slight beam flange trimming) was also proposed recently [8]. The aim is, based on the capacity design concept, to move the plastic hinging of the beam away from the face of the column so that the more vulnerable welded joints are effectively protected. Among a variety of improved moment connections, welding a triangular haunch with a structural tee shape beneath the beam has been shown to be very effective for repair, rehabilitation, or new construction [5,6]. However, the labor cost for fitting a triangular haunch connection (Fig. 1) is expensive. In addition, the complete joint penetration groove weld at both ends of the haunch flange with an inclined angle

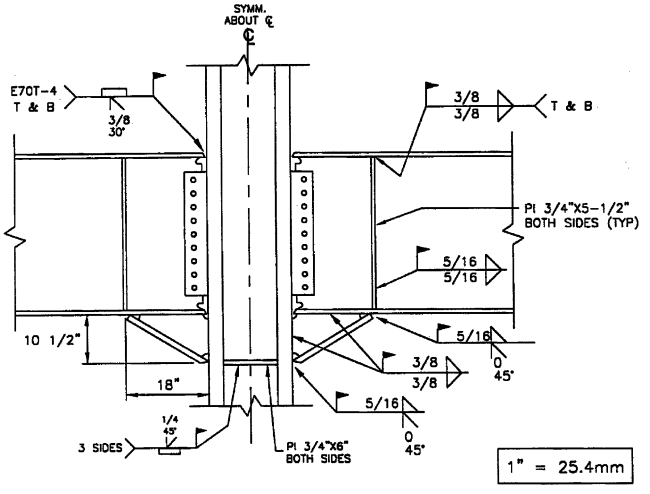

Fig. 1. Welded triangular haunch connection (Uang et al. [5]).

* Corresponding author. Tel.: +82-2-880-8735; fax: +82-2-871-5518.
E-mail address: ceholee@snu.ac.kr (C.-H. Lee).

0141-0296/$ - see front matter © 2003 Elsevier Ltd. All rights reserved.
doi:10.1016/S0141-0296(03)00176-7

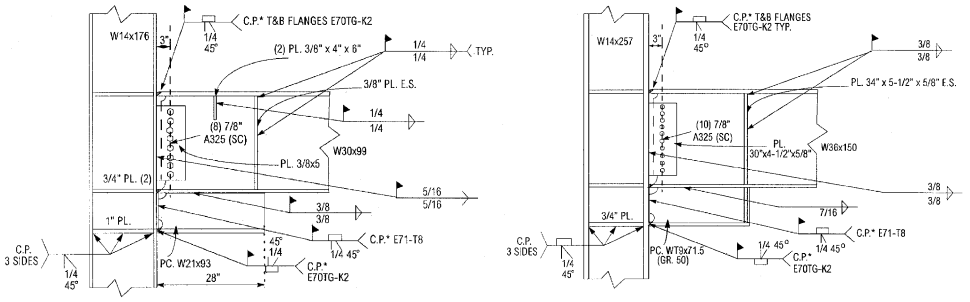

Fig. 2. Welded straight haunch test specimens (SAC [9]), (a) UCSD test specimen, (b) UCB test specimen.

requires a significant amount of overhead welding. To minimize the construction cost, the use of a straight haunch with one free end has been proposed by the SAC Joint Venture [9].

In Phase 1 of the SAC Joint Venture, cyclic testing of two full-scale straight haunch moment connections was conducted at UCSD and UCB with the details shown in Fig. 2. The failure modes of the two test specimens are shown in Fig. 3. In the UCSD specimen, weld fractures initiated from the haunch tip, where stress concentration was the highest. Once the haunch was completely separated from the beam, the beam top flange groove weld experienced brittle fracture. In this connection, only 0.02 rad plastic rotation was achieved. In the UCB specimen, a pair of beam web stiffeners was extended to the haunch web to prevent the fracture of fillet welds at the haunch tip. However, the beam top flange fractured across the entire width near the flange weld after considerable yielding of the connection. The maximum plastic rotation achieved in the UCB specimen was only 0.015 rad. Both specimens performed unsatisfactorily and no further test was conducted. Recently, based on the finite element analysis results, a design procedure and a simplified analytical model that considers the force interaction and deformation compatibility between the beam and haunch were proposed [10]. In this follow-up study, cyclic seismic testing was conducted to verify the proposed procedure and to develop schemes that would prevent cracking at the haunch tip.

2. Brief summary of previous study

A previous study by Lee and Uang [10] found that the welded haunch drastically changed the force transfer mechanism that could not be predicted reliably by the beam theory. Unlike the expectation from the classical beam theory, an inclined strip in the web of the straight haunch acted as a strut (Fig. 4). Both high shear and normal stresses exist at the interface between the beam and haunch. High stress concentration was also evident

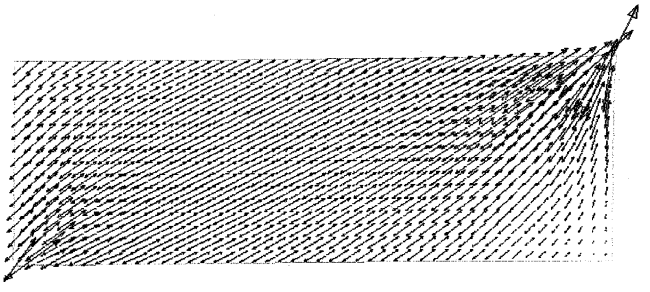

Fig. 4. Principal stress distribution in haunch web (Lee and Uang [10]).

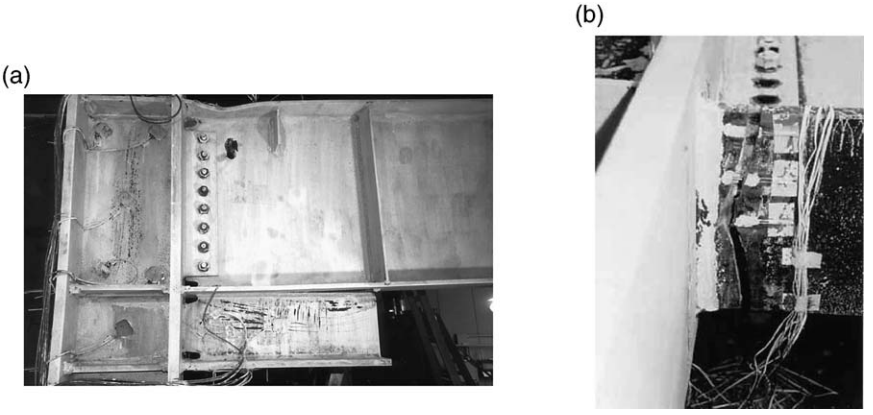

Fig. 3. Failure modes of SAC test specimens (SAC [9]), (a) Haunch tip cracking of UCSD specimen, (b) Beam top flange fracture of UCB specimen.

at the upper corner, where unzipping of fillet welds was observed during testing. To some extent, the web of the straight haunch could be viewed as a vertical rib plate. The flange of the straight haunch was not highly stressed, but it also served as a stiffener to stabilize the haunch web. Fig. 5 shows a simplified analytical model that considers the force interaction and deformation compatibility between the beam and haunch. In the proposed model, the haunch web and the haunch flange were idealized as a four-node rectangular plane stress finite element and a truss element, respectively. By idealizing the profiles of the stresses at the interface, both shear and normal interaction forces can be determined from the conditions of force equilibrium and deformation compatibility. Knowing these interaction forces reduces the remaining design problem into a simple statics one. A design procedure as well as several schemes that minimize the stress concentration at the haunch tip was also recommended in the previous study.

3. Testing program

3.1. Design of test specimens

Fig. 6 shows a portion of the moment frame using a welded straight haunch. Following the capacity design

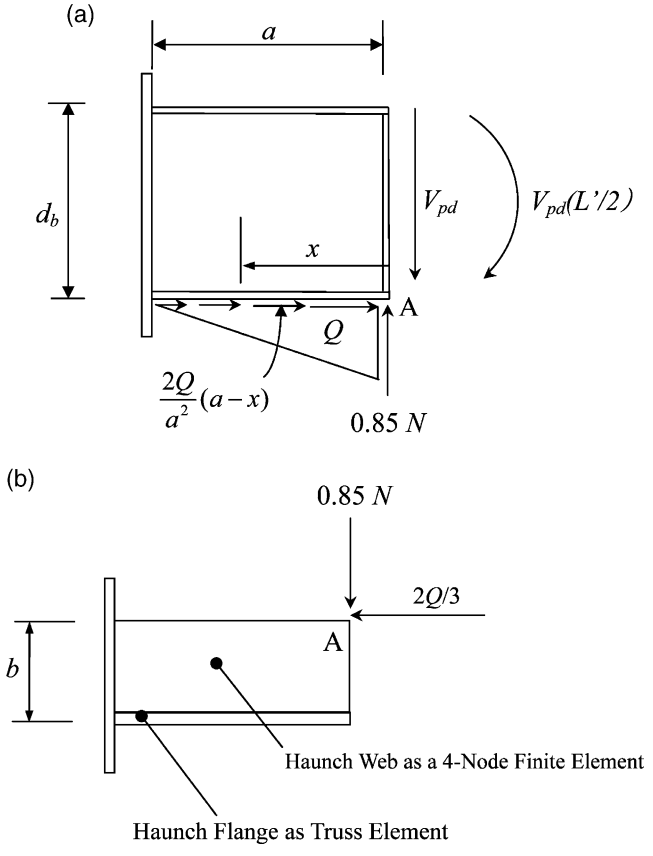

Fig. 5. Simplified interaction model between beam and haunch (Lee and Uang [10]), (a) Beam, (b) Haunch.

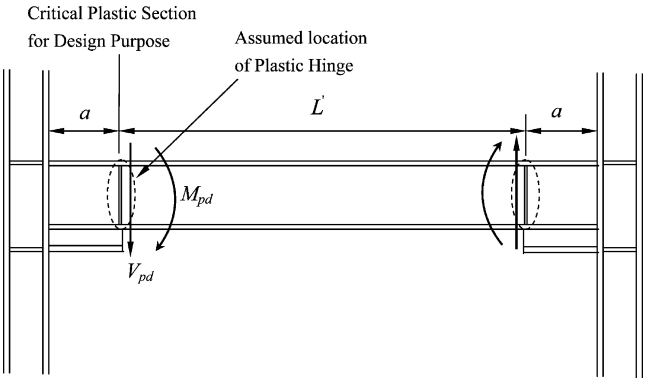

Fig. 6. Typical beam span with welded straight haunch.

concept, the aim of haunch strengthening was to effectively move the plastic hinging of the beam outside the haunch region such that the haunch region remains essentially elastic.

Specimens were designed by following the design procedure according to Lee and Uang [10], the American Institute of Steel Construction (AISC) *seismic provisions* [11], and the *LRFD specification* [12]. Detailed design calculations are omitted here due to space limitations. Table 1 summarizes the results for each design step. An exterior moment connection was designed with the following data: story height H_c = 3600 mm; bay width = 7200 mm; haunch length a = 600 mm; haunch depth b = 220 mm; distance between haunch tip L' = 6000 mm; beam H-600X200X11X17 (SS400 steel, F_y = 236 MPa, F_{ye} = 314 MPa); column H-400X408X21X21 (SM490 steel, F_{yc} = 325 MPa); haunch web and flange plate (SM490 steel, F_y = 325 MPa); and filler metal with a specified CVN value of 26.7 J (20 ft-lb) at −28.9 °C (−20 °F) was used (F_{EXX} = 492 MPa).

Other than using steel backing bars, ceramic backing bars were used to construct the notch-free groove weld joint more economically. Cosmetic fillet welds were then added after removing the ceramic backing bars. Weld access hole detail recommended in SAC (2000) [13] was utilized for the straight haunch specimens. The beam web was groove welded to the column flange and the haunch web was fillet welded to both the column and the beam flanges. The majority of the normal force N at the beam–haunch interface is concentrated near the haunch tip (see Fig. 5). A pair of transverse stiffeners was added to the beam web at the haunch tip location. The stiffeners were designed per Chapter K of the AISC *LRFD specification* [12] for local web yielding and web crippling. Continuity plates were not provided at the beam bottom flange level because flexural stress level there was very low [10]. A total of four test specimens were fabricated. The connection detail drawings are illustrated in Figs. 7–10. Specimen PN600-SB (Fig. 7) was fabricated as a bench mark specimen by following typical pre-Northridge (PN) moment connection details.

Table 1
Summary of test specimen design

Design step	Calculations
Preliminary haunch sizing (20 and 21)[a]	Assume $a \approx d_b$ = 600 mm, $b \approx a\tan(20^o) \approx 220$ mm. Try WT built-up from two 20 × 200 mm plates; A_T = 8000 mm^2, A_{hf} = 4000 mm^2, I_T = 37 670 000 mm^4, b_1 = 55 mm, b_2 = 65 mm, t_{hf} = 20 mm, t_{hw} = 20 mm.
Beam design moment and shear (22 and 23)	$M_{pd} = 1.1Z_bF_{ye}$ = 1024 kN m, $V_{pd} = 2M_{pd}/L'$ = 341 kN
Strong column–weak beam condition (24)	$\Sigma M^*_{pc}/\Sigma M^*_{pb}$ = (2375 kN m/1002 kN m) = 2.37 > 1.0
Interaction forces (11 and 12)	N = 588 kN, Q = 1646 kN
Check flexural stresses at the groove welds (17, 19, and 20)	f_{tf}(beam top flange) = 359 MPa < $F_w = F_{EXX}$ = 490 MPa, f_{hf} (haunch flange) = 283 MPa
Check flexural haunch strength and compactness (28 and 30)	$t_{hw} = 20 \text{ mm} > \dfrac{\sqrt{(Q - f_{hf}A_{hf})^2 + 3N^2}}{b(\phi F_y)} = 18$ mm, $b_{hf}/(2t_{hf}) = 5.0 < 137/\sqrt{F_y} = 7.6$, $b/t_{hw} = 11.0 < 683/\sqrt{F_y} = 37.9$
Design haunch fillet welds (32 and 34)	(i) Fillet weld (two-sided) between the haunch web and beam: $S > 10$ mm, use 12 mm fillet weld. (ii) Fillet weld (two-sided) between the haunch web and column flange: $S > 13$ mm, use 15 mm fillet weld. (iii) Fillet weld (two-sided) between the haunch web and haunch flange: $\phi(0.6F_{EXX})(0.707S \times 2a) \geq f_{hf}A_{hf}$; $S > 7$ mm, use 10 mm fillet weld.
Design of beam web stiffeners	Taking the "effective" bearing length near the haunch tip as (0.1)a: $\phi R_n = 1.0(2.5k + 0.10a)F_yt_{bw}$ = 408 kN < N=588 kN (NG). Try a pair of 10 × 80 mm plates (SM490 steel) for the stiffeners. The width–thickness ratio is acceptable. Treat the stiffened web as an axially compressed member with an effective length of 0.75h (h = 566 mm) (AISC 1993). ϕ_cP_n = 832 kN > N=588 kN (OK). Use two-sided 6 mm fillet welds to connect the stiffeners to the beam web.

[a] Relevant equation numbers in the previous study (Lee and Uang [10]).

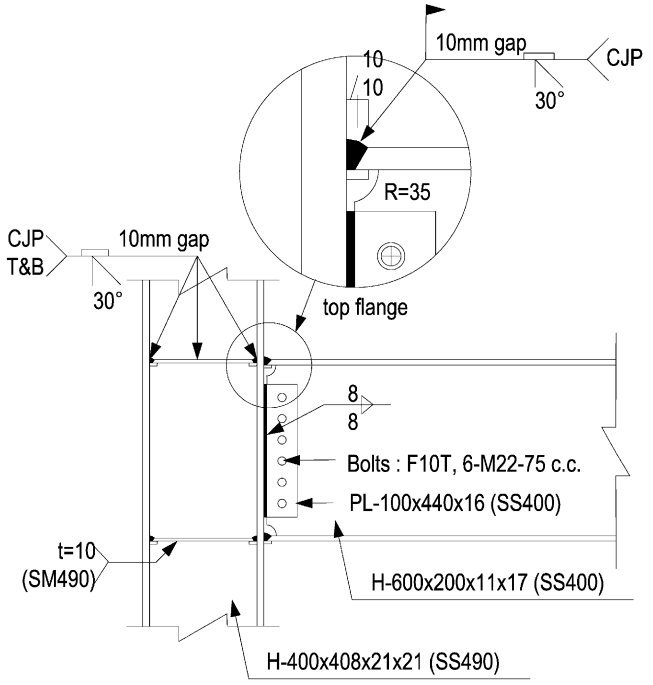

Fig. 7. Specimen PN600-SB.

The three haunch specimens were nominally identical except for the haunch tip details that were used to avoid cracking of the fillet welds at the haunch tip. A tapered end combined with a drilled hole near the haunch tip was provided in specimen SH600-H & T (Fig. 8). In specimen SH600-H & PE (Fig. 9), a pair of partially extended beam web stiffeners with drilled holes near the haunch tip was provided. A pair of beam web stiffeners was fully extended to the haunch flange in specimen SH600-FE (Fig. 10). Thus, specimen SH600-FE had the largest degree of restraint and redundancy at the haunch tip among the three haunch specimens.

3.2. Test setup and loading

The specimens were mounted to the strong floor and strong wall. An overall view of the test setup is shown in Fig. 11. Specimens were tested statically according to the SAC 2000 standard seismic loading protocol as shown in Fig. 12 [13]. A servo-controlled actuator, capable of applying loads up to 980 kN and displacements of up to ±250 mm was used. The beam tip displacement corresponding to the story drift ratio of 1% was 38 mm. Lateral restraints were provided at a distance of 2150 and 3160 mm from the column face. Specimens were instrumented with a combination of displacement transducers, strain gage rosettes and uniaxial strain gages to measure global and local responses. Whitewash was also painted around the connection to monitor the deformation during the test.

4. Test results and discussions

4.1. Global response

Tensile test results for the coupons cut from the test specimens are summarized in Table 2. The cyclic responses in terms of the total plastic rotation are presented in Fig. 13. The ordinate is expressed in terms

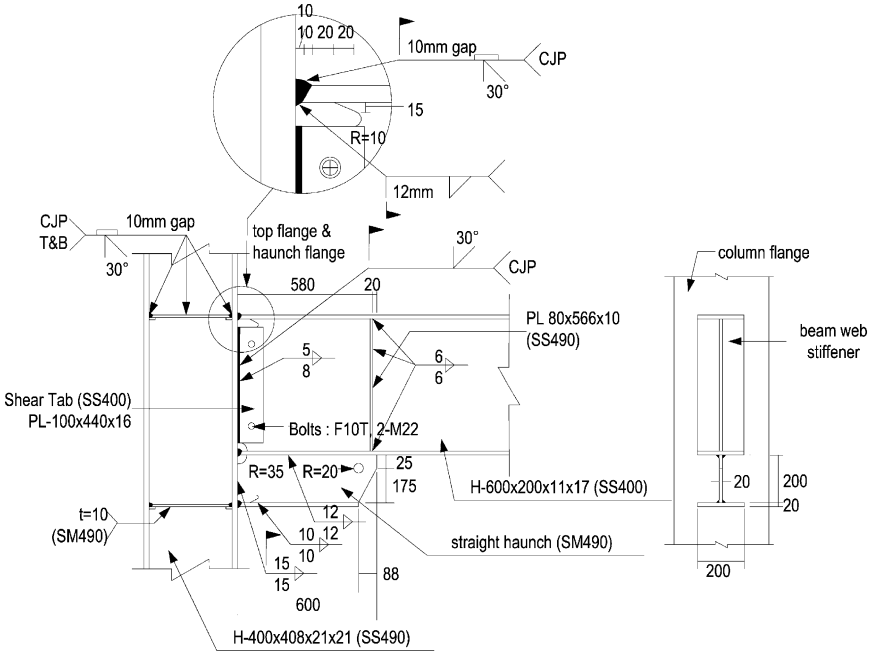

Fig. 8. Specimen SH600-H & T.

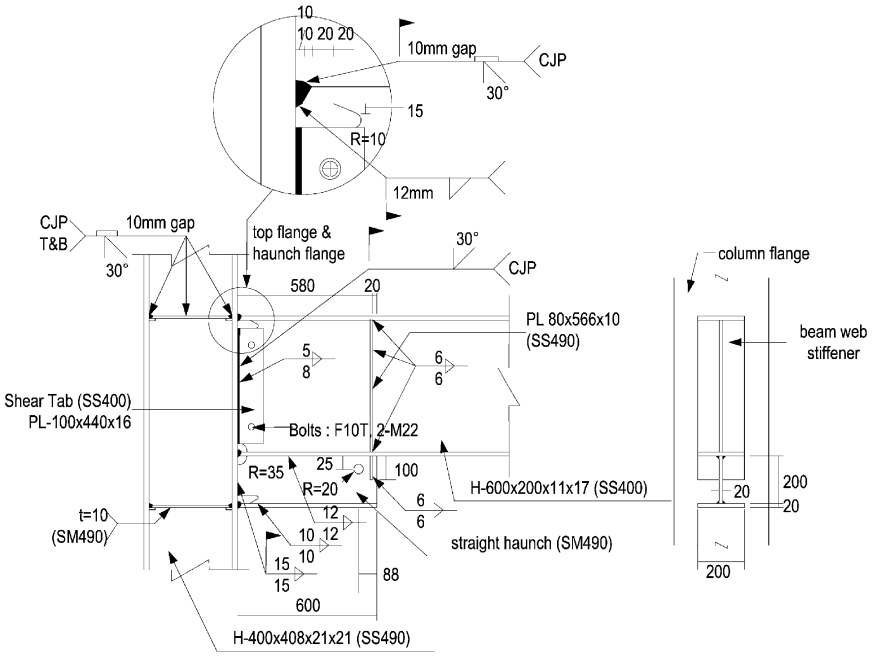

Fig. 9. Specimen SH600-H & PE.

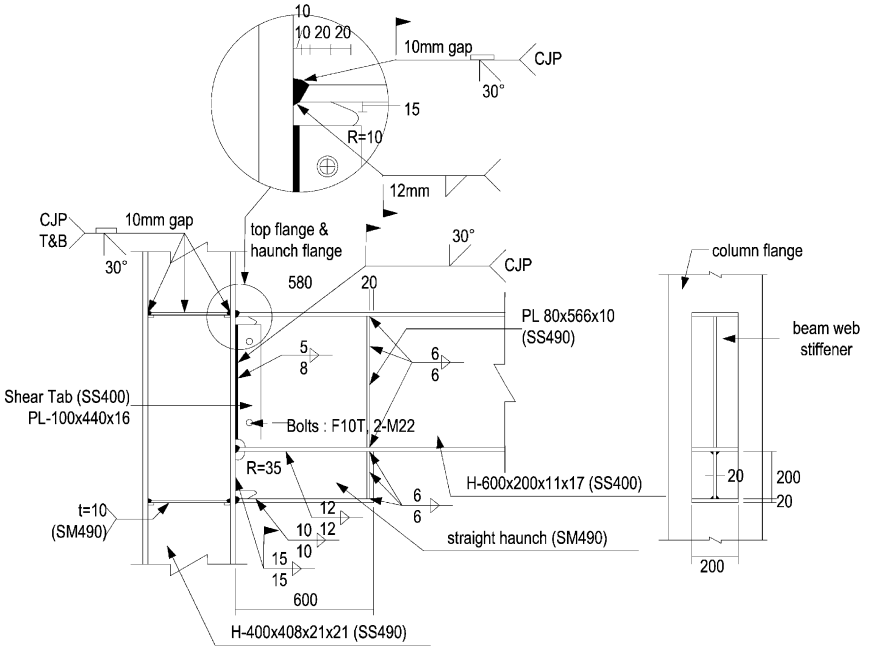

Fig. 10. Specimen SH600-FE.

of the normalized moment M/M_p, where M and M_p are the moment at the column face and the beam plastic moment based on measured yield stress, respectively. The plastic rotation was computed by dividing the plastic beam tip displacement by the distance from the beam tip to the column face. All haunch specimens exhibited satisfactory levels of connection ductility required of special moment frames. No haunch specimen exhibited fracture during the test. After one cycle loading of the 5% story drift, testing was terminated due to severe lateral twist. As seen in Fig. 14, the presence of the haunch effectively moved the plastic hinging of the beam outside the haunch region as intended in the design of specimens. The maximum flexural strain level measured near the haunch tip of specimen SH600-FE was about eight times the yield strain. A sloped edge combined with a drilled hole near the haunch tip, or a pair of stiffeners partially or fully extended from the beam web, success-

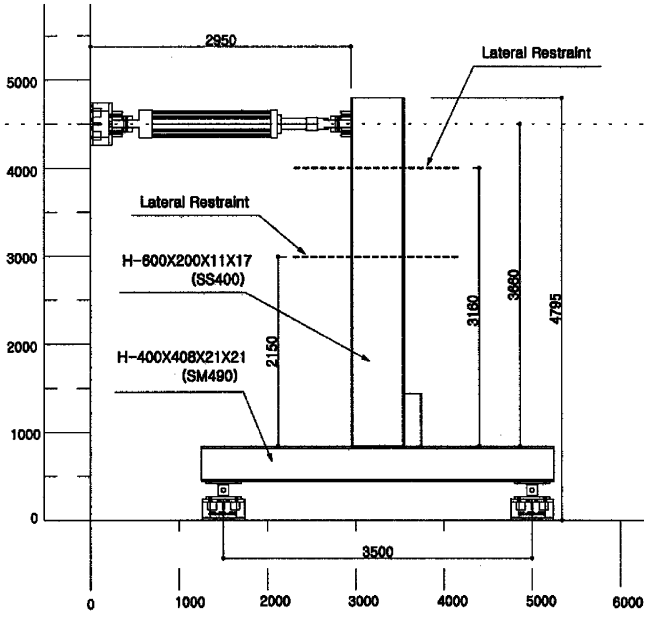

Fig. 11. Test setup.

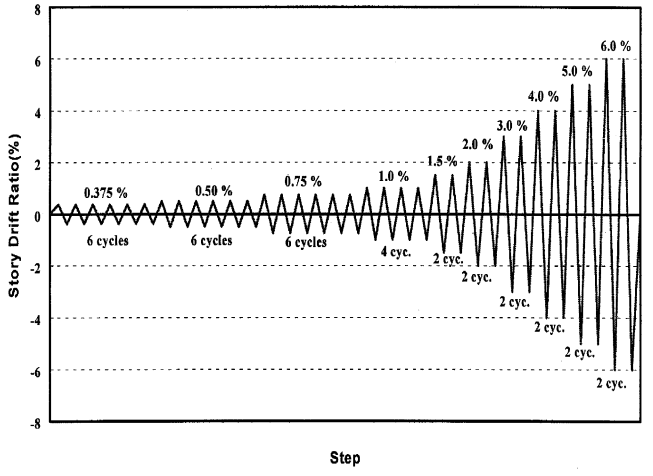

Fig. 12. SAC standard seismic loading protocol (SAC [13]).

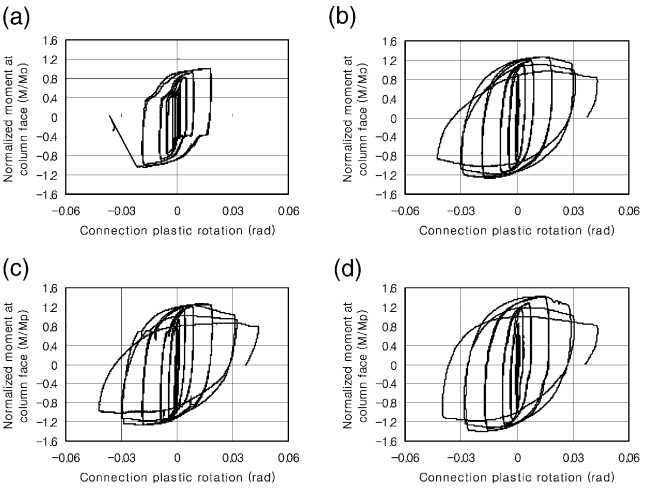

Fig. 13. Moment versus connection plastic rotation relationships, (a) PN500-5B, (b) SH600-H&T, (c) SH600-H&PE, (d) SH600-FE.

fully prevented crack initiation at the haunch tip. The pre-Northridge type specimen PN600-SB showed premature brittle fracture of the beam top flange (Fig. 15). Neglecting the slippage component of the base block that occurred during the test, the connection plastic rotation achieved in this specimen was only 0.012 rad. Fig. 16 illustrates the comparison of dissipated energy. Each haunch specimen dissipated a similar amount of energy (about 530 kN m). The strain hardening factor, computed using Eq. (1) at the haunch tip based on the measured yield stress, reached a maximum value of about 1.1 at the 3% story drift response (Fig. 17).

$$\alpha = \frac{M_{\text{tip}}}{Z_{\text{f}} \times F_{\text{yf}} + Z_{\text{w}} \times F_{\text{yw}}} \tag{1}$$

where M_{tip} is the measured moment at the haunch tip, Z_{f}, Z_{w}, the beam flange and beam web plastic section modulus, respectively and F_{yf}, F_{yw}, is the beam flange and beam web yield stress obtained from tension coupon test, respectively (Table 2). This value is comparable to that recommended by the AISC seismic provision [11].

Table 2
Tensile coupon test results

Test coupon	F_{y} (N/mm^2)	F_{u} (N/mm^2)	Elong.[a] (%)	Yield ratio (%)
Beam flange (SS400)	309	439	32	70
Beam web (SS400)	335	449	29	75
Column flange (SM490)	379	557	26	68
Column web (SM490)	377	554	24	68
Haunch web (SM490)	343	538	28	64
Haunch flange (SM490)	346	538	27	64

[a] Based on gage length of 200 mm.

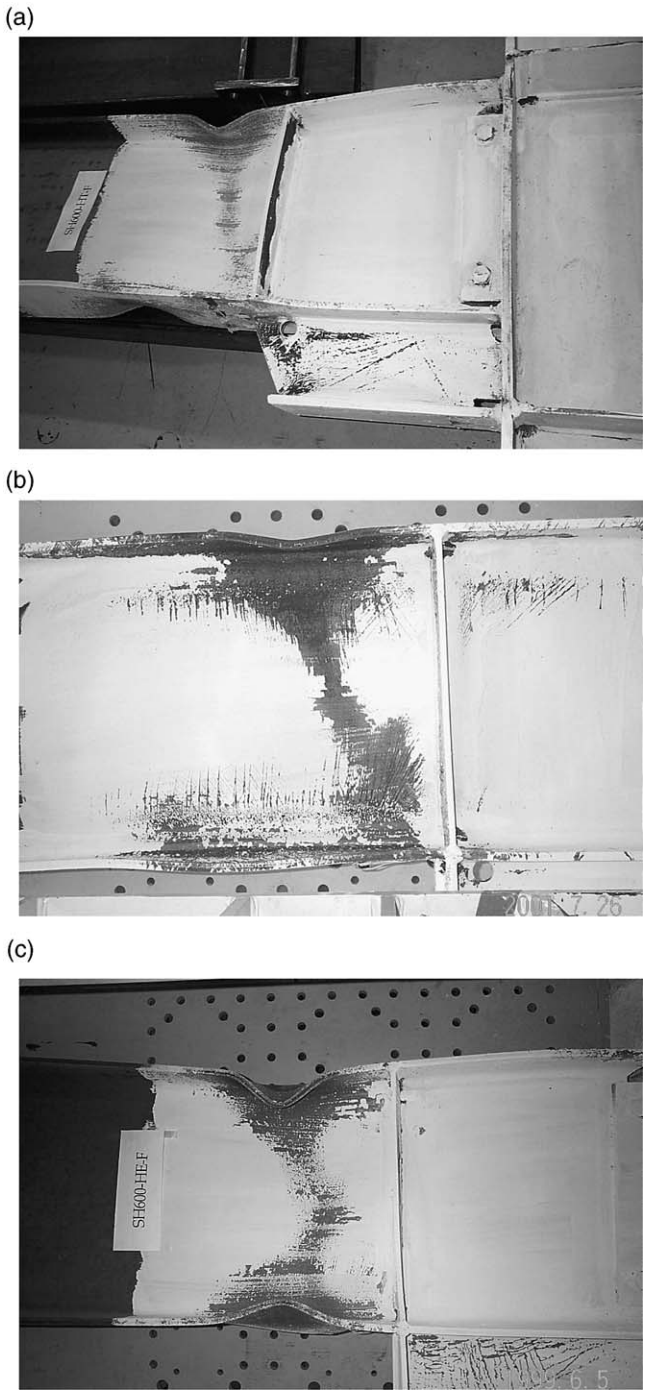

Fig. 14. Plastic hinging of straight haunch specimens, (a) SH600-H&T, (b) SH600-H&PE, (c) SH600-FE.

Fig. 15. Brittle fracture of beam top flange (specimen PN600-SB).

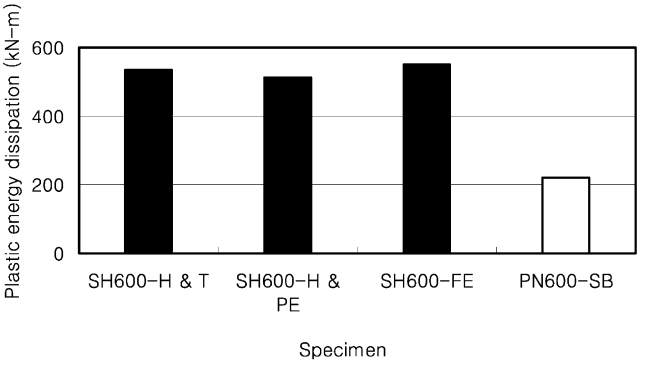

Fig. 16. Comparison of energy dissipation.

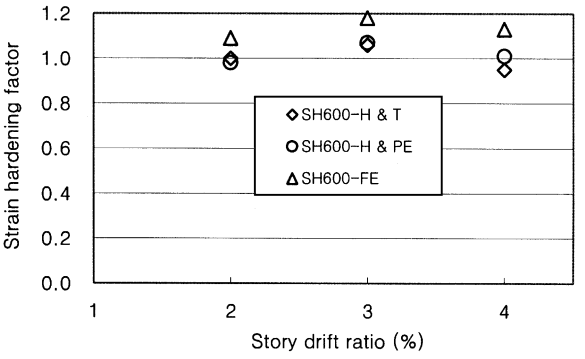

Fig. 17. Story drift ratio versus strain hardening factor.

Fig. 18 presents cyclic shear strain responses measured at the center of the upper and lower panel zones. From this figure, it can be seen that both the upper and lower panel zones responded elastically and that the upper panel zone was subjected to a higher shear strain demand; with the presence of a haunch two panel zones that form an enlarged (or dual) panel zone are created, and therefore the panel zone strength becomes higher [14].

4.2. Buckling behavior

Fig. 19 compares the cyclic response envelopes of the three haunch specimens. It is noted that the connection strength degraded at a faster rate in positive moment (or the beam top flange compression loading) after the 3% story drift cycle. Table 3 summarizes the measured buckling amplitudes at the 4% story drift cycle. The web local buckling (WLB) amplitudes did not show appreciable difference, regardless of the sign of the bending moment. The flange local buckling (FLB) amplitudes

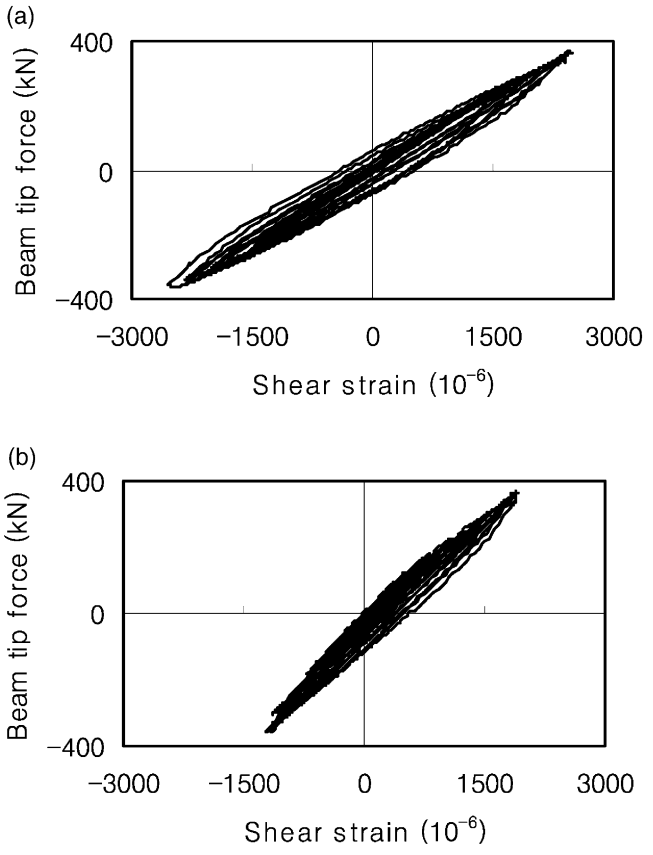

Fig. 18. Cyclic shear strain responses measured at the center of the upper and lower panel zones (specimen SH600-FE), (a) upper panel zone, (b) lower panel zone.

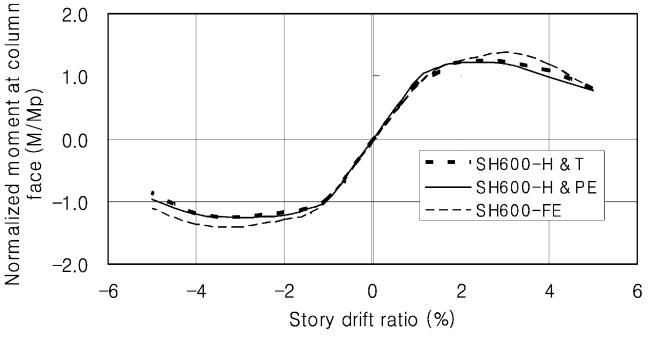

Fig. 19. Comparison of response envelopes.

were smaller in negative bending (or the beam bottom flange compression loading). This seemed to have been caused by a shorter buckling length of the beam bottom flange due to the restraint provided by the haunch. It can be observed from Table 3 that the lateral torsional buckling (LTB) amplitudes changed drastically depending on both the sign of the bending moment and the haunch tip details. In negative bending, the haunches of specimens SH600-H & PE and SH600-FE were effective in providing restraint to the beam bottom flange, thereby decreasing the LTB and FLB amplitudes in proportion to the degree of the haunch tip restraint. It is noted again that the haunch tip of specimen SH600-FE had the largest degree of bracing and restraint effects to the beam bottom flange. However, in positive bending, the reverse was observed, i.e., the LTB amplitudes increased as the degree of the haunch tip restraint increased. This implies that the presence of a haunch beneath the beam bottom flange does not provide any bracing effects to the beam top flange. On the contrary, as the haunch tip restraint increased, the center of twisting of the integral section of the beam and haunch appeared to shift downward. However, considering that continuous lateral bracing to the top flange is usually provided by a composite floor slab, such a large LTB in positive moment as observed in these bare steel specimens will not be a design issue.

Table 3
Buckling amplitudes at 4% story drift cycle

Specimen	LTB (cm)	WLB (cm)	FLB (cm)
(a) Beam top flange compression (positive bending)			
SH600-H & T	5.0	3.0	4.0
SH600-H & PE	7.0	5.0	5.5
SH600-FE	8.0	4.0	4.0
(b) Beam bottom flange compression (negative bending)			
SH600-H & T	5.0	4.5	3.5
SH600-H & PE	3.0	4.0	2.5
SH600-FE	2.5	3.0	2.0

4.3. Strut action, neutral axis location, and connection stiffness

The previous study predicted that, contrary to the classical beam theory, an inclined strip in the web of the straight haunch would act as a strut. The principal strain directions were calculated based on the strain rosette measurements (Table 4). The results show that the web of the straight haunch acted as a strut with an inclined angle of about 30° throughout the response.

It was also predicted that the neutral axis only shifts slightly downward in the haunch region as a result of the strut action of the haunch web. Fig. 20 shows the strain gage locations and the measured cyclic flexural responses along the depth of the beam and haunch. Positive loading corresponds to the beam top flange compression. The measured flexural strain data from GAGES 1–3 appeared unusual; the data shifted slightly to the compression side. It is not clear whether this was caused by an instrumentation problem. But the data were still considered useful in locating the neutral axis experimentally. If the classical beam theory which treats the beam and haunch as an integral section holds, the neutral axis should shift downward almost to the location of GAGE 5 (or 130 mm away from the beam bottom flange). How-

Table 4
Angle of principal strain measured at haunch web (specimen SH600-H & PE)

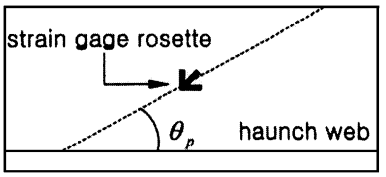

Story drift ratio (%)	Strain ($\times 10^{-6}$)					θ_p (°)
	ε_x	$\varepsilon_{45°}$	ε_y	γ_{xy}	ε_p	
0.75	−267	−397	135	662	−453	29.4
1	−289	−478	156	823	−535	30.8
1.5	−321	−569	176	993	−629	31.7
2	−300	−580	199	1059	−636	32.4
3	−244	−592	166	1106	−629	34.8

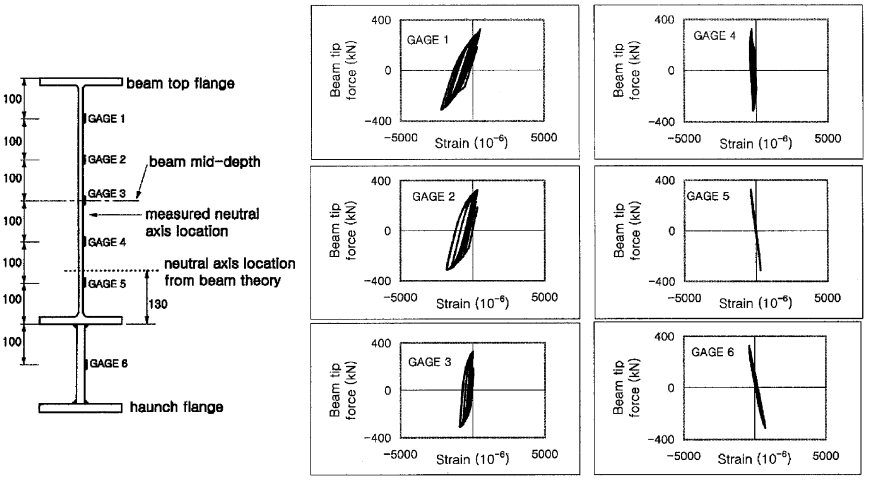

Fig. 20. Cyclic flexural strain responses along beam depth (SH600-H & PE).

ever, it is observed from Fig. 20 that the global sign of the cyclic response changed somewhere between GAGE 3 and 4. This means that the neutral axis only shifts slightly downward as predicted in the previous study and that the beam theory no longer holds.

When a haunch is added beneath the beam, the panel zone is enlarged (or the dual panel zone is formed) and the beam portion within the haunch region is reinforced. As a side effect, increase in frame lateral stiffness is expected. Fig. 21 shows the comparison of the measured elastic lateral stiffness. It is observed that about 25% increase in frame lateral stiffness resulted from this one-sided haunch reinforcement as a side effect.

5. Conclusions

The main conclusions on cyclic seismic testing of steel moment connections reinforced with welded straight haunch are summarized as follows:

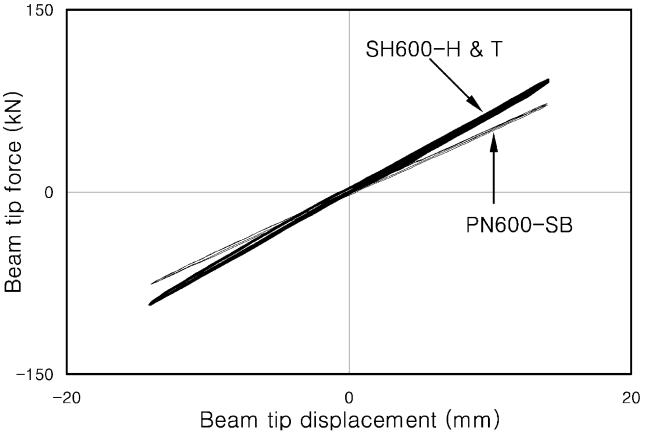

Fig. 21. Comparison of measured elastic lateral stiffness (SH600-H & T versus PN600-SB).

1. The straight haunch specimens designed by the method proposed in the previous study effectively moved the plastic hinging of the beam away from the haunch tip and developed satisfactory levels of connection ductility without fracture. The strain gage readings from the test confirmed that an inclined strip in the web of the straight haunch acts as a strut and that the neutral axis only shifts slightly downward as a result of the strut action.
2. A sloped edge combined with a drilled hole near the haunch tip, and a pair of stiffeners partially or fully extended from the beam web, successfully prevented fracture at the haunch tip. Test results confirmed that continuity plates are not needed at the beam bottom flange level because of low flexural stress in that area.
3. The haunch was effective in providing restraint to the beam bottom flange in negative bending, thereby decreasing the LTB and FLB amplitudes in proportion to the degree of the haunch tip fixity. However, in positive bending, the presence of the haunch beneath the beam did not provide any bracing effects.

References

[1] Chen SJ, Yeh CH, Chu JM. Ductile steel beam-to-column connections for seismic resistance. J Struct Eng, ASCE 1996;122(11):1292–9.
[2] Plumier A. The dogbone: back to the future. Eng J 1997;34(2):61–7.
[3] Zekioglu A, Mozaffarian H, Chang KL, Uang C-M. Designing after Northridge. Modern Steel Constr 1997;37(3):36–42.
[4] Engelhardt MD, Winneberger T, Zekany AJ, Potyraj TJ. Experimental investigations of dogbone moment connections. Eng J 1998;35(4):128–39 [AISC, Fourth Quarter].
[5] Uang C-M, Yu Q-S, Noel S, Gross J. Cyclic testing of steel moment connections rehabilitated with RBS or welded haunch. J Struct Eng, ASCE 2000;126(1):57–68.
[6] Yu Q-S, Uang C-M, Gross J. Seismic rehabilitation design of steel moment connection with welded haunch. J Struct Eng, ASCE 2000;126(1):69–78.
[7] Kim T, Whittaker AS, Gilani ASJ, Bertero VV, Takhirov SM. Experimental evaluation of plate-reinforced steel moment-resisting connections. J Struct Eng, ASCE 2002;128(4):483–91.
[8] Lee C-H. Seismic design of rib-reinforced steel moment connections based on equivalent strut model. J Struct Eng 2002;128(9):1121–9.
[9] SAC. Experimental investigations of beam–column subassemblies. Report No. SAC-96-01. SAC Joint Venture, Sacramento, Calif., 1996.
[10] Lee C-H, Uang C-M. Analytical modeling and seismic design of steel moment connections with welded straight haunch. J Struct Eng 2001;127(9):1028–35.
[11] AISC. Seismic provisions for structural steel buildings. 2nd ed. Chicago, IL: AISC; 1997.
[12] AISC. Load and resistance factor design specification. 2nd ed. Chicago: AISC; 1993.
[13] SAC. Seismic design criteria for new moment-resisting steel frame construction. Report No. FEMA 350. SAC Joint Venture, Sacramento, Calif., 2000.
[14] Lee C-H, Uang C-M. Analytical modeling of dual panel zone in haunch repaired steel MRFs. J Struct Eng 1997;23(1):20–9.